Dependence of nuclear binding on hadronic mass variation

V. V. Flambaum[1,2] and R. B. Wiringa[1]

[1]*Physics Division, Argonne National Laboratory, Argonne, Illinois 60439, USA*
[2]*School of Physics, University of New South Wales, Sydney 2052, Australia*
(Received 1 September 2007; published 12 November 2007)

We examine how the binding of light ($A \leqslant 8$) nuclei depends on possible variations of hadronic masses, including meson, nucleon, and nucleon-resonance masses. Small variations in hadronic masses may have occurred over time; the present results can help evaluate the consequences for big bang nucleosynthesis. Larger variations may be relevant to current attempts to extrapolate properties of nucleon-nucleon interactions from lattice QCD calculations. Results are presented as derivatives of the energy with respect to the different masses so they can be combined with different predictions of the hadronic mass-dependence on the underlying current-quark mass m_q. As an example, we employ a particular set of relations obtained from a study of hadron masses and sigma terms based on Dyson-Schwinger equations and a Poincaré-covariant Faddeev equation for confined quarks and diquarks. We find that nuclear binding decreases moderately rapidly as the quark mass increases, with the deuteron becoming unbound when the pion mass is increased by ~60% (corresponding to an increase in $X_q = m_q/\Lambda_{\rm QCD}$ of 2.5). In the other direction, the dineutron becomes bound if the pion mass is decreased by ~15% (corresponding to a reduction of X_q by ~30%). If we interpret the disagreement between big bang nucleosynthesis calculations and measurements to be the result of variation in X_q, we obtain an estimate $\delta X_q/X_q = K \cdot (0.013 \pm 0.002)$ where $K \sim 1$ (the expected accuracy in K is about a factor of 2). The result is dominated by ^{7}Li data.

PACS number(s): 21.10.Dr, 21.45.+v, 26.35.+c, 98.80.Cq

I. INTRODUCTION

There are several reasons to search for a variation of the fundamental "constants" of nature in space and time. First, the Universe is evolving; several phase transitions happened in the early Universe accompanied by dramatic changes in vacuum energy, fundamental masses, fundamental interactions (electromagnetic, weak, and strong) and properties of elementary particles (e.g., confinement of quarks). At later stages the equation of state of the Universe continued to evolve, from radiation domination (pressure $p = \epsilon/3$ where ϵ is the energy density), to cold-matter domination ($p \ll \epsilon$), and "recently", about five billion years ago, to dark-energy domination ($p \approx -\epsilon$). In view of these dramatic changes it seems natural to check if there is any evolution in the values of the fundamental constants during this process.

A second reason is that spatial variation can explain a fine-tuning of the fundamental constants which allows humans (and any life) to appear. Indeed, it is well-known that if the values of some fundamental constants (e.g., related to the strong interaction) would differ by even 1% we could not appear. If we assume that the fundamental constants vary in space, this problem of fine-tuning may be resolved in a most natural way: we appeared in the area of the Universe where the values of the fundamental constants are consistent with our existence.

A third reason comes from theories unifying gravity and other interactions. Some theories suggest the possibility of spatial and temporal variation of physical "constants" in the Universe (see, e.g., [1–8]). Moreover, there exists a mechanism for making all coupling constants and masses of elementary particles both space- and time-dependent, and influenced by local circumstances. The variation of coupling constants can be nonmonotonic (e.g., damped oscillations).

We can only measure the variation of dimensionless parameters which do not depend on the units we use. In the Standard Model the two most important dimensionless parameters are the fine structure constant $\alpha = e^2/\hbar c$ and the ratio of the electroweak unification scale (determined by the Higgs vacuum expectation value) to the quantum chromodynamics (QCD) scale $\Lambda_{\rm QCD}$ [defined as the position of the Landau pole in the logarithm for the running strong coupling constant, $\alpha_s(r) \sim {\rm const}/\ln{(\Lambda_{\rm QCD} r/\hbar c)}$]. The variation of the Higgs vacuum expectation value (VEV) leads to the variation of the electron mass m_e and quark mass m_q which are proportional to the Higgs VEV. The present work considers effects produced by the variation of $X_q = m_q/\Lambda_{\rm QCD}$ where $m_q = (m_u + m_d)/2$ is the average current-quark mass.

Up to now a majority of publications about temporal and spatial variation of the fundamental constants have considered effects of variation of α. However, the hypothetical unification of all interactions implies that the variation of the strong interaction parameter $X_q = m_q/\Lambda_{\rm QCD}$ may be larger than the variation of the electromagnetic α. For example, the grand unification theories (GUTs) discussed in Ref. [1] predict

$$\frac{\delta X_q}{X_q} \sim 35 \frac{\delta \alpha}{\alpha}. \tag{1}$$

The coefficient here is model-dependent but large values are generic for grand unification models in which variations come from high energy scales; they appear because the running strong-coupling constant and Higgs constants (related to mass) run faster than α. Indeed, the electroweak ($i = 1,2$) and strong ($i = 3$) inverse coupling constants have the following dependence on the scale ν and normalization point ν_0:

$$\alpha_i^{-1}(\nu) = \alpha_i^{-1}(\nu_0) + b_i \ln(\nu/\nu_0). \tag{2}$$

In the Standard Model, $2\pi b_{i=1,2,3} = 41/10, -19/6, -7$; the electromagnetic $\alpha^{-1} = (5/3)\alpha_1^{-1} + \alpha_2^{-1}$ and the strong $\alpha_s = \alpha_3$. In GUTs all coupling constants are equal at the unification scale, $\alpha_i(\nu_0) \equiv \alpha_{\text{GUT}}$. We may consider two possibilities: if we assume that only α_{GUT} varies, then Eq. (2) gives us the same shifts for all inverse couplings:

$$\delta\alpha_1^{-1} = \delta\alpha_2^{-1} = \delta\alpha_3^{-1} = \delta\alpha_{\text{GUT}}^{-1}. \quad (3)$$

We see that the variation of the strong interaction constant $\alpha_3(\nu)$ at low energy ν is much larger than the variation of the electromagnetic constant α, since $\delta\alpha_3/\alpha_3 = (\alpha_3/\alpha_{1,2})\delta\alpha_{1,2}/\alpha_{1,2}$ and $\alpha_3 \gg \alpha_{1,2}$.

The second possibility is the variation of the GUT scale [ν/ν_0 in Eq. (2)]. This gives

$$\delta\alpha_1^{-1}/b_1 = \delta\alpha_2^{-1}/b_2 = \delta\alpha_3^{-1}/b_3. \quad (4)$$

Note that in this case the variations have different signs since b_1 and $b_{2,3}$ have different signs. However, we expect an even larger enhancement of the variation of α_3 ($\delta\alpha_3/\alpha_3 = (b_3\alpha_3/b_{1,2}\alpha_{1,2})\delta\alpha_{1,2}/\alpha_{1,2})$.

The variation of m/Λ_{QCD} can be estimated from the definition of Λ_{QCD}. The running of α_s near the electroweak scale is given by

$$\alpha_s(\nu)^{-1} \approx b_s \ln(\nu/\Lambda_{\text{QCD}}). \quad (5)$$

Let us take $\nu = m_z$ where m_z is the Z-boson mass. The variation of Eq. (5) and relations above give

$$\frac{\delta(m_z/\Lambda_{\text{QCD}})}{(m_z/\Lambda_{\text{QCD}})} = -\frac{1}{b_s\alpha_s(m_z)}\frac{\delta\alpha_s(m_z)}{\alpha_s(m_z)} \sim \frac{C}{\alpha(m_z)}\frac{\delta\alpha(m_z)}{\alpha(m_z)}. \quad (6)$$

The value of the constant C here depends on the model used. However, the enhancement $1/\alpha \sim 100$ should make the factor C/α large. Note that m_z (as well as $m_{e,q}$) is proportional to the Higgs VEV.

If this estimate is correct, the variation in $m_{e,q}/\Lambda_{\text{QCD}}$ may be easier to detect than the variation in α. The cosmological variation of m_q/Λ_{QCD} can be extracted from the big bang nucleosynthesis (BBN), quasar absorption spectra and Oklo natural nuclear reactor data [9]. For example, the factor of three disagreement between the calculations and measurements of the BBN abundance of ^{7}Li may, in principle, be explained by the variation of m_q/Λ_{QCD} at the level of $\sim 10^{-3}$–10^{-2} [10] (see also recent work [11–13]). The claim of the variation of the fundamental constants based on the Oklo data in Ref. [14] is not confirmed by recent studies [15] which give a stringent limit on the possible variation of the resonance in ^{150}Sm during the last two billion years. The search for the variation of m_e/Λ_{QCD} using the quasar absorption spectra gave a nonzero result in Ref. [16] but zero results in Refs. [17,18]. The present time variation of $m_{e,q}/\Lambda_{\text{QCD}}$ can be extracted from comparison of different atomic [19] and nuclear [20,21] clocks. The review of the recent results on the variation of α, m_e/Λ_{QCD} and m_q/Λ_{QCD} can be found in Ref. [22].

As we mentioned above, one can measure the variation of the dimensionless parameter $X_q = m_q/\Lambda_{\text{QCD}}$. Note that $m_q \approx 4$ MeV $\ll \Lambda_{\text{QCD}} \approx 220$ MeV. As a result, nuclear parameters (nucleon mass, reaction cross sections, etc.) are determined mainly by Λ_{QCD}. Therefore, in all calculations it is convenient to assume that Λ_{QCD} is constant and calculate the dependence

on the small parameter m_q. In other words, we measure all masses in units of Λ_{QCD} and will simply restore Λ_{QCD} in the final results. For example, the relation between the variation of the proton mass and quark mass $\delta m_p/m_p = 0.064\delta m_q/m_q$ should be understood as $\delta X_p/X_p = 0.064\delta X_q/X_q$ where $X_p = m_p/\Lambda_{\text{QCD}}$ and $X_q = m_q/\Lambda_{\text{QCD}}$. This approach was formulated in Ref. [9].

Predictions for the relations between the variations of quark and hadron masses may come from a variety of approaches, such as chiral perturbation theory [23–26] or Dyson-Schwinger equations (DSE) [27,28]. Nuclear binding energies and spectra would vary as a consequence of the hadron mass variation, affecting a number of physical processes, such as BBN and the Oklo phenomenon. Large enough changes might alter the stability of some nuclei, e.g., unbind the deuteron, bind the dineutron, or even make $A = 5, 8$ nuclei particle-stable [29]. In this work we estimate the changes in binding for $A = 2$–8 nuclei that result from small changes in hadronic masses. We also evaluate the effect of much larger changes on the two-nucleon systems, which may be relevant to present attempts to extrapolate results from lattice QCD calculations [30]. We first consider how changes in meson, nucleon, and nucleon-resonance masses would alter some representative nucleon-nucleon (NN) Hamiltonians. We then solve for the energy of the two-body systems exactly and calculate variational Monte Carlo (VMC) estimates for the larger nuclei with these forces. We report our results as derivatives of the energies with respect to the different hadron mass changes, so that the results can be utilized with different predictions of the coordinated changes between quark and hadron masses. Finally, we utilize the DSE predictions for hadron mass-dependence on the quark mass as an example to explore the effects on nuclear spectra and BBN.

II. NUCLEAR HAMILTONIAN

We examine several Hamiltonians of the form

$$H = \sum_i K_i + \sum_{i<j} v_{ij} + \sum_{i<j<k} V_{ijk}. \quad (7)$$

Here K_i is a nonrelativistic kinetic energy operator, v_{ij} is a two-nucleon potential, and V_{ijk} is a possible three-nucleon potential. We consider three different Argonne models for v_{ij}: Argonne v_{14} (AV14) and Argonne v_{28} (AV28) from 1984 [31], and Argonne v_{18} (AV18) from 1995 [32]. In conjunction with AV18, we will use the Urbana model IX (UIX) V_{ijk} from 1995 [33].

The AV14 and AV18 models are conventional NN potentials, while the AV28 model has additional explicit $\Delta(1232)$ degrees of freedom. The AV14 and AV28 were constructed together and fit to the same np phase-shift solution WI81 of Arndt and Roper [34] so they are phase equivalent. The intention was to use them in parallel many-body calculations to study the effect of including explicit Δ's in the nuclear Hamiltonian. In practice, AV28 has proven difficult to use, so beyond the two-nucleon system, only some triton [35] and nuclear matter [36] calculations have been reported. However, AV14 has been widely used in a variety of few-body [37,38]

and dense nucleon matter [39] calculations. The AV18 is an updated version of AV14 containing charge-independence-breaking (CIB) terms and a complete electromagnetic interaction. AV18 was fit directly to 4301 pp and np data in the 1993 Nijmegen partial-wave analysis [40], and AV18 and AV18+UIX have become standard Hamiltonians for *ab initio* calculations of light nuclei [41] and dense matter [42].

All three of the Argonne potentials contain electromagnetic (EM) interaction, long-range one-pion-exchange (OPE), intermediate-range attraction, and short-range repulsion, written as a sum of operator components:

$$v_{ij} = v_\gamma(r_{ij}) + \sum_p \left[v_\pi^p(r_{ij}) + v_I^p(r_{ij}) + v_S^p(r_{ij}) \right] O_{ij}^p. \quad (8)$$

The number of operators O_{ij}^p is 14, 28, or 18, as indicated by the AVxx designation. The different operators are discussed in detail below; here we summarize the differences between the models. The AV14 and AV28 potentials both use an average nucleon mass, while AV18 keeps separate proton and neutron masses, which introduces a small charge-symmetry-breaking (CSB) term into K_i. The K_i for AV28 also depends explicitly on the Δ mass. In AV14 and AV28, v_γ is just the Coulomb interaction between protons (with a form factor); in AV18 the magnetic moment interaction, vacuum polarization, and other small EM terms are added.

The NN part of OPE is the same in AV14 and AV28, and an average pion mass is used. In AV18 there is a weaker OPE coupling strength, a slightly different form factor, and the small charge-dependent (CD) terms owing to the difference between neutral and charged pion masses are kept. The intermediate-range attraction is due primarily to two-pion-exchange (TPE) processes; in AV14 and AV18 this feature is approximated by using the square of the OPE tensor function $T(m_\pi r)$ as a phenomenological radial shape for v_I^p and adjusting strength parameters of the 14 or 18 operators to fit data. In AV28, 14 operators with explicit NN–$N\Delta$–$\Delta\Delta$ couplings are added to those of AV14; twelve of these have OPE range and two have intermediate and short range. These produce much of the intermediate-range attraction explicitly through coupled-channel effects. The coefficients of the first 14 NN operators are refit to the data but are smaller in magnitude than in AV14.

The short-range repulsion may be attributed to the exchange of heavier ρ and ω mesons with suitable form factors for finite-size effects, but in all the Argonne models it is treated phenomenologically. AV14 and AV28 use a Woods-Saxon radial shape with 14 strength parameters while AV18 has a slightly more general shape with 26 parameters.

A. Potentials

The OPE potential between nucleons can be written as

$$v_\pi(r_{ij}) = f_{\pi NN}^2 [X_{ij} \tau_i \cdot \tau_j + \tilde{X}_{ij} T_{ij}]. \quad (9)$$

Here $T_{ij} = 3\tau_{zi}\tau_{zj} - \tau_i \cdot \tau_j$ is the CD isotensor operator which contributes when the difference between neutral and charged pion masses is retained, and

$$X_{ij} = \frac{1}{3}\left(X_{ij}^0 + 2X_{ij}^\pm \right), \quad (10)$$

$$\tilde{X}_{ij} = \frac{1}{3}\left(X_{ij}^0 - X_{ij}^\pm \right), \quad (11)$$

$$X_{ij}^m = \left(\frac{m}{m_s} \right)^2 \frac{1}{3} mc^2 [Y(mr_{ij})\sigma_i \cdot \sigma_j + T(mr_{ij})S_{ij}]. \quad (12)$$

The $S_{ij} = 3\sigma_i \cdot \hat{r}_{ij}\sigma_j \cdot \hat{r}_{ij} - \sigma_i \cdot \sigma_j$ is the usual tensor operator and $Y(mr)$ and $T(mr)$ are the normal Yukawa and tensor functions

$$Y(mr) = \frac{e^{-\mu r}}{\mu r}\xi(r), \quad (13)$$

$$T(mr) = \left(1 + \frac{3}{\mu r} + \frac{3}{(\mu r)^2} \right) Y(mr)\xi(r), \quad (14)$$

where $\mu = mc/\hbar$ and a short-range form factor $\xi(r)$ has been incorporated that makes both $Y(mr)$ and $T(mr)$ vanish linearly at the origin. In AV18, the $X^{0,\pm}$ are calculated with explicit m_{π^0} and $m_{\pi^\pm}$ masses and the scaling mass $m_s \equiv m_{\pi^\pm}$. In AV14 and AV28 an average $m_\pi = \frac{1}{3}(m_{\pi^0} + 2m_{\pi^\pm})$ is used, so that $\tilde{X}_{ij}$ vanishes, and the scaling mass $m_s \equiv m_\pi$. The coupling $f_{\pi NN}^2 = 0.081$ in AV14 and AV28, and 0.075 in the more modern AV18.

The intermediate-range and short-range terms in the potentials are given by

$$v_I^p(r_{ij}) = I^p T^2(m_\pi r), \quad (15)$$

$$v_S^p(r_{ij}) = (S^p + Q^p r + R^p r^2)W(r), \quad (16)$$

where $W(r)$ is a Woods-Saxon function. For AV14 and AV28, $Q^p = R^p = 0$, while in AV18, there are boundary conditions on v^p such that no more than two of the three S^p, Q^p, and R^p are independent and free to be fitted for any given operator. The associated operators O_{ij}^p include 14 charge-independent (CI) operators that are common to all the models:

$$O_{ij}^{p=1,14} = [1, \sigma_i \cdot \sigma_j, S_{ij}, \mathbf{L} \cdot \mathbf{S}, \mathbf{L}^2, \mathbf{L}^2(\sigma_i \cdot \sigma_j), (\mathbf{L} \cdot \mathbf{S})^2]$$
$$\otimes [1, \tau_i \cdot \tau_j]. \quad (17)$$

Here $\mathbf{L}$ is the relative orbital angular momentum and $\mathbf{S}$ is the total spin of the pair. The AV18 model has four additional CD and CSB terms:

$$O_{ij}^{p=15,18} = [1, \sigma_i \cdot \sigma_j, S_{ij}] \otimes T_{ij}, \quad (\tau_{zi} + \tau_{zj}). \quad (18)$$

These latter terms are small, but important for fitting the differences between current pp and np scattering data.

There are fourteen additional operators in AV28 that involve explicit Δ degrees of freedom. The first two are

$$O_{ij}^{p=15} = (\sigma_i \cdot \mathbf{S}_j)(\tau_i \cdot \mathbf{T}_j) + (\mathbf{S}_i \cdot \sigma_j)(\mathbf{T}_i \cdot \tau_j) + \text{H.c.}, \quad (19)$$

$$O_{ij}^{p=16} = S_{ij}^{II}(\tau_i \cdot \mathbf{T}_j) + S_{ji}^{II}(\mathbf{T}_i \cdot \tau_j) + \text{H.c.}, \quad (20)$$

where $\mathbf{S}_i$ ($\mathbf{T}_i$) is the transition spin (isospin) operator for particle i that changes a spin (isospin) $\frac{1}{2}$ state to a $\frac{3}{2}$ state. The generalized tensor operator is $S_{ij}^{II} = 3\sigma_i \cdot \hat{r}_{ij}\mathbf{S}_j \cdot \hat{r}_{ij} - \sigma_i \cdot \mathbf{S}_j$ and H.c. denotes the Hermitian conjugate. These operators are part of a generalized OPE contribution

$$v_\pi^{II}(r_{ij}) = f_{\pi NN} f_{\pi N\Delta} \left(\frac{m}{m_s} \right)^2 \frac{1}{3} mc^2 [Y(mr_{ij})O_{ij}^{15}$$
$$+ T(mr_{ij})O_{ij}^{16}] \quad (21)$$

that produces NN–$N\Delta$ transitions. The $\pi N\Delta$ vertex coupling is taken as $f_{\pi N\Delta} = 2f_{\pi NN}$. Other operators provide OPE contributions to NN–$\Delta\Delta$, $N\Delta$–ΔN, $N\Delta$–$N\Delta$, $N\Delta$–$\Delta\Delta$, and $\Delta\Delta$–$\Delta\Delta$ transitions, with an additional coupling $f_{\pi\Delta\Delta} = \frac{1}{5}f_{\pi NN}$ being introduced. Intermediate- and short-range interaction is also added in the diagonal $N\Delta$–$N\Delta$ and $\Delta\Delta$–$\Delta\Delta$ channels. The full set of operators is detailed in Ref. [31].

The Urbana model of three-nucleon interaction (TNI) is written as a sum of two-pion-exchange P-wave and remaining shorter-range phenomenological terms,

$$V_{ijk} = V_{ijk}^{2\pi,P} + V_{ijk}^{R}. \tag{22}$$

The structure of the TPE P-wave term is expressed simply as

$$V_{ijk}^{2\pi,P} = \sum_{cyc} \left(A_{2\pi}^{P} \left\{ X_{ij}^{m}, X_{jk}^{m} \right\} \{ \tau_i \cdot \tau_j, \tau_j \cdot \tau_k \} \right.$$
$$\left. + C_{2\pi}^{P} \left[X_{ij}^{m}, X_{jk}^{m} \right] [\tau_i \cdot \tau_j, \tau_j \cdot \tau_k] \right), \tag{23}$$

where X_{ij}^{m} is the same spin-space function of Eq. (12) evaluated with the average pion mass, $\sum_{cyc}$ is a sum over the three cyclic exchanges of nucleons i, j, and k, and $C_{2\pi}^{P} = \frac{1}{4}A_{2\pi}^{P}$. The $A_{2\pi}^{P}$ and the strength of the V_{ijk}^{R} term are determined by fitting the binding energy of ^{3}H [33] and the saturation density of nuclear matter [42] in the presence of a given v_{ij}; the parameters of UIX were selected in conjunction with AV18.

B. Dependence on hadron masses

We consider changes in the Hamiltonian that would be induced by small changes in the hadron masses. However, we do not consider changes in the coupling constants that might occur due to mass-dependent loop corrections [23,24]. Variations of the nucleon and nucleon-resonance masses alter the kinetic energy operator:

$$K_i = -\frac{\hbar^2}{2m_i}\nabla_i^2 + (m_i - m_N)c^2, \tag{24}$$

where m_i is the average nucleon mass $m_N = \frac{1}{2}(m_p + m_n)$ for AV14, but may be m_Δ part of the time for AV28. For AV18 the kinetic energy operator has no m_Δ component, but does include a small CSB piece:

$$K_i = -\frac{\hbar^2}{2m_N}\nabla_i^2 - \frac{\hbar^2}{2m_N}\left(\frac{m_n - m_p}{m_n + m_p}\right)\tau_{zi}\nabla_i^2, \tag{25}$$

where $m_N = 2m_p m_n/(m_p + m_n)$. There is also a small dependence on the nucleon mass in the magnetic moment parts of the EM interaction in AV18.

Changes in m_N and m_Δ also affect the energy expectation value for AV28 through effects of the NN–$N\Delta$–$\Delta\Delta$ coupled channels. This can be visualized in a simple closure approximation (see Eq. (33) of Ref. [31] and the accompanying discussion) for the TPE diagrams where one or two intermediate Δ's are excited, propagate, and then deexcited by the transition

potentials:

$$V_{\text{eff}} \approx 2V_{NN-N\Delta}\frac{-1}{\bar{E}_1 + (m_\Delta - m_N)}V_{N\Delta-NN}$$
$$+ V_{NN-\Delta\Delta}\frac{-1}{\bar{E}_2 + 2(m_\Delta - m_N)}V_{\Delta\Delta-NN}. \tag{26}$$

The two mean-energy denominators $\bar{E}_1$ and $\bar{E}_2$ would vary, in part, as the kinetic energies of the intermediate states:

$$\bar{E}_1 \approx \frac{\hbar^2\bar{k}^2}{2m_N} + \frac{\hbar^2\bar{k}^2}{2m_\Delta}, \tag{27}$$

$$\bar{E}_2 \approx 2\frac{\hbar^2\bar{k}^2}{2m_\Delta}, \tag{28}$$

with $\bar{k}$ an average intermediate momentum. This physical effect can be approximated in the AV14 and AV18 potentials by multiplying the intermediate-range strength coefficients I^p of Eq. (15) by factors $(1 + \delta_N)$ and $(1 + \delta_\Delta)$. The above equations represent only some of the terms contributing to the m_N and m_Δ dependence introduced by the coupled channels, so we will fix the δ_N and δ_Δ terms for AV14 by requiring that calculated two-body energies have the same mass dependence as AV28 without these factors. We will take the same factors as approximately correct modifications for AV18 also.

The dependence on the pion mass (which vanishes in the chiral limit $m_q = 0$) can be obtained from the original pion-exchange interaction which is proportional to the second derivative of the exponential potential, $\nabla_i\nabla_j[\exp(-\mu r)/r]$—see, e.g., Ref. [9]. As a result, the variation of the pion mass affects the strength of the OPE through the m^3 dependence of X_{ij}^{m} in Eq. (12) and through the range of the Yukawa functions $Y(mr)$ and $T(mr)$, Eqs. (13) and (14). Note that the scaling mass m_s is not allowed to vary (this is only a coefficient which does not vanish in the chiral limit $m_q = 0$). The dependence of OPE terms on pion mass is thus the same as given in Eq. (10) of Ref. [23]. Neglecting the small effect of our short-range form factor $\xi(r)$, the function $m^3 Y(mr)$ has a constant volume integral. If m is increased, $m^3 Y(mr)$ will be larger inside $r = 2/\mu$ and smaller outside. However, $m^3 T(mr)$ will be smaller at all values of $r > 0$.

The generalized OPE of AV28 that couples to intermediate $N\Delta$ and $\Delta\Delta$ states effectively incorporates considerable multipion exchange effects. We can approximate this real physical effect in AV14 and AV18 by assuming the intermediate-range potential has the mass-dependence $v_I^p(r) \propto [m_\pi^3 T(m_\pi r)]^2$. The closure approximation of Eq. (26) that justifies this connection applies most clearly to the first six static (**L**-independent) operators O_{ij}^p of Eq. (17) because of the closed algebra of the spin (isospin) and transition-spin (isospin) operators. However, the **L**-dependent operators can also be affected through the coupled-channels, so we will also consider changing these terms in the intermediate-range potentials. We will also consider changes to the residual $v_I^p(r)$ terms in AV28. Thus we will study variations attributable to the pion mass in four stages with our Hamiltonians: (1) change in the OPE part of the potential v_π (and v_π^{II}, etc., for AV28) only; (2) change in both v_π and the static TPE parts $v_I^{p=1,6}$ (TPE-s); (3) these changes plus the **L**-dependent TPE parts

$v_I^{p=7,14}$ (TPE-L); and (4) these changes in v_{ij} plus the TPE part of the three-nucleon potential $V_{ijk}^{2\pi,P}$ (TNI).

Representing the dependence on heavier meson masses $m_\rho \approx m_\omega \approx m_V$ is much more problematic because the Argonne models do not have explicit heavy-meson exchange. However, the effect of a short-range interaction is determined mostly by the volume integral of this interaction, e.g., the volume integral gives us the strength constant B if we want to approximate a short-range interaction by a zero-range interaction $B\delta(\mathbf{r})$. Therefore, we may approximate the dependence on masses of heavier mesons by a change in the range parameters r_0 and a of the short-range Woods-Saxon potential

$$W(r) = \frac{1}{1 + \exp[(r - r_0)/a]} \quad (29)$$

used in Eq. (16). To keep the same relative variation of the volume integral for the Woods-Saxon potential and the meson exchange potential $\exp(-m_V r)/r$ we change the parameters at the rate

$$\frac{\delta r_0}{r_0} = \frac{\delta a}{a} = -\frac{2}{3}\frac{\delta m_V}{m_V}. \quad (30)$$

In this case, as m_V increases, the range of the Woods-Saxon decreases while the value at the origin remains constant and the volume integral varies as m_V^{-2}.

The repulsive core of the three-nucleon potential V_{ijk}^R may be attributed to a combination of multi-pion and heavy-meson exchanges, and also some relativistic effects [43]. Owing to its complicated nature and phenomenological treatment and the fact that it gives a small contribution to energy expectation values, we do not attempt to determine its variation with changes in the hadronic masses.

III. ENERGY CALCULATIONS

We calculate the energies of the $^1S_0(np)$ virtual bound state and the deuteron for AV28, AV14, and AV18 by direct solution of the two-body equations. The energies of ^{3}H, ^{3,4,5}He, ^{6,7}Li, and ^{7,8}Be are calculated for AV14 and AV18+UIX using variational Monte Carlo (VMC) methods. The VMC method is described in detail in Ref. [41] and references therein. Briefly, we construct suitably parametrized trial wave functions Ψ_V and evaluate the upper bound to the ground-state energy,

$$E_V = \frac{\langle \Psi_V | H | \Psi_V \rangle}{\langle \Psi_V | \Psi_V \rangle} \geqslant E_0, \quad (31)$$

using Monte Carlo techniques for the multi-dimensional integration. The parameters in Ψ_V are varied to minimize E_V,

and the lowest value is taken as the approximate solution. We use a variational wave function of the form

$$|\Psi_V\rangle = \left[1 + \sum_{i<j<k} U_{ijk}^{TNI}\right]\left[\mathcal{S}\prod_{i<j}(1 + U_{ij})\right]|\Psi_J\rangle. \quad (32)$$

The U_{ij} and U_{ijk}^{TNI} are noncommuting two- and three-nucleon correlation operators, reflecting the spatial and operator dependence of v_{ij} and V_{ijk}, and $\mathcal{S}$ is a symmetrization operator. The form of the antisymmetric Jastrow wave function Ψ_J depends on the nuclear state under investigation. For the s-shell nuclei the simple form

$$|\Psi_J\rangle = \prod_{i<j} f_c(r_{ij})|\Phi_A(JMTT_3)\rangle \quad (33)$$

is used. Here the $f_c(r_{ij})$ are central (spin-isospin independent) two-body correlation functions and Φ_A is an antisymmetrized spin-isospin state, e.g.,

$$|\Phi_4(0000)\rangle = \mathcal{A}|\uparrow p \downarrow p \uparrow n \downarrow n\rangle, \quad (34)$$

with $\mathcal{A}$ the antisymmetrization operator. The Ψ_J for p-shell nuclei is more complicated; details are given in Ref. [41]. The two-body correlation operator U_{ij} is a sum of spin, isospin, and tensor terms:

$$U_{ij} = \sum_{p=2,6} u_p(r_{ij})O_{ij}^p, \quad (35)$$

where the O_{ij}^p are the static operators of Eq. (17). The central $f_c(r)$ and noncentral $u_p(r)$ pair correlation functions are generated by a set of six coupled, Schrödinger-like, differential equations which include the v_{ij} and a number of embedded variational parameters. These parameters are optimized in the energy minimization and then kept fixed as the hadronic masses are varied. The correlations are adjusted, however, because the altered interaction is used to regenerate the correlations in each case.

The energies we obtain are shown in Table I and compared to experiment. The VMC method is reasonably accurate for s-shell nuclei, giving energies ∼2–3% less bound than exact methods like Faddeev or Green's function Monte Carlo for a given Hamiltonian [41]. It is not as good for p-shell binding energies, but many other features such as density distributions and electromagnetic moments are in good agreement. We anticipate that small changes in the binding energies induced by small changes in hadron masses will be accurately tracked with the VMC calculations. The comparison between AV14 and AV18+UIX models indicates the importance of including a three-nucleon interaction to approach the experimental energies.

TABLE I. Ground state energies of light nuclei in MeV for the different Hamiltonians used in this work compared to experiment.

	$^1S_0(np)$	^{2}H	^{3}H	^{3}He	^{4}He	^{5}He	^{6}Li	^{7}Li	^{7}Be	^{8}Be
AV28	0.0661	−2.2250								
AV14	0.0663	−2.2250	−7.50	−6.88	−23.60	−21.26	−24.31	−28.31	−26.85	−40.26
AV18+UIX	0.0665	−2.2246	−8.25	−7.49	−27.50	−25.26	−28.22	−33.33	−31.74	−48.63
Expt.		−2.2246	−8.48	−7.72	−28.30	−27.41	−31.99	−39.24	−37.60	−56.50

TABLE II. Dimensionless derivatives $\Delta\mathcal{E}(m_H) = \frac{\delta E/E}{\delta m_H/m_H}$ of the energy for the $^1S_0(np)$ virtual bound state ϵ_v and the deuteron Q for all three Hamiltonians.

m_H	$\Delta\epsilon_v$			ΔQ		
	AV28	AV14	AV18	AV28	AV14	AV18
m_N	−88.1	−32.6	−33.4	13.06	8.63	8.90
$m_N + \delta_N$		−91.2	−121.2		13.03	17.82
m_Δ	63.9			−5.15		
δ_Δ		68.1	102.2		−5.12	−10.36
m_π (OPE)	9.5	−4.1	−3.8	−2.23	−1.55	−1.40
m_π (+TPE-s)	24.4	35.5	53.0	−3.63	−4.02	−6.70
m_π (+TPE-L)				−4.02	−4.31	−6.74
m_V	−153.7	−245.0	−381.9	20.88	22.92	41.74

We evaluate the mass-dependence of the energies of the two- and multinucleon systems by changing the hadron masses m_H one at a time, increasing the value by 0.1% and calculating the resulting energy, and then decreasing by 0.1% and repeating the energy calculation. The VMC calculations follow the same random walk stored from the initial energy evaluation to reduce the contribution of statistical noise. Results given in the following three tables are the dimensionless derivatives of the energy with respect to changes in the hadron masses

$$\Delta\mathcal{E}(m_H) = \frac{\delta E/E}{\delta m_H/m_H}. \quad (36)$$

These results can then be combined with any given model for how the different hadron masses are correlated with the underlying quark masses to give a total binding energy prediction:

$$E(m_q) = E(m_{q_0})\left[1 + \sum_{m_H}\Delta\mathcal{E}(m_H)\frac{\delta m_H(m_q)}{m_H}\right], \quad (37)$$

where m_{q_0} is the physical current-quark mass. A specific example will be given below.

A. Two-nucleon energies

The two-nucleon results for $\Delta\mathcal{E}(m_H)$ are given in Table II for all three Hamiltonians. A simple approximate relation between changes in the deuteron binding energy Q and virtual bound state energy ϵ_v is given by [10]

$$\frac{\Delta\epsilon_v(m_H)}{\Delta Q(m_H)} \approx -\frac{\sqrt{Q}}{\sqrt{\epsilon_v}}. \quad (38)$$

Despite the wide range of values for $\Delta\mathcal{E}(m_H)$ in Table II, this relation is valid within a factor of ∼2 for fifteen out of seventeen pairs of results. The two exceptions are for the OPE components of $\Delta\epsilon_v(m_\pi)$ for AV14 and AV18, where the sign is incorrect. This discrepancy will be discussed below.

Changing the nucleon mass in AV14 and AV18 primarily changes just the kinetic energy component and is very similar for the two models: a larger m_N translates to smaller $\langle K \rangle$ and more binding and thus a positive derivative $\Delta Q(m_N)$ for the deuteron. For the virtual bound state, the effect is the same but

greater attraction corresponds to a reduction in the magnitude of ϵ_v and a negative $\Delta\epsilon_v(m_N)$.

Changing m_N in AV28 produces a larger change in the energies due to the additional coupled-channel effects of Eqs. (26)–(27) discussed above. The change is more dramatic for ϵ_v than for Q, probably because the $^1S_0$ NN channel can couple to both $N\Delta$ and $\Delta\Delta$ intermediate states, while the deuteron can have only NN and $\Delta\Delta$ components due to isospin conservation. To approximately incorporate this physical effect into the phase-equivalent AV14 model, we can multiply its intermediate-range strength parameters I^p of Eq. (15) by a factor $(1 + \delta_N)$. We choose a value $\delta_N = 0.49\delta m_N/m_N$ that matches the mass dependence in the deuteron as shown by the line in Table II labeled "$m_N + \delta_N$". This same factor approximately fixes the virtual bound state also. Using the same δ_N factor in AV18 produces a change about one third larger. This difference is probably due to the fact that AV18 is fit to a more recent data set, with a weaker OPE coupling accompanied by more-attractive intermediate-range terms and correspondingly more-repulsive short-range terms.

Increasing the Δ mass in AV28 reduces the binding energy both through the one-body term of Eq. (24) and through the coupled-channel effects of Eq. (26). Thus $\Delta\mathcal{E}(m_\Delta)$ has a sign opposite to $\Delta\mathcal{E}(m_N)$. To approximate this affect for AV14, we can again multiply its intermediate-range strength parameters I^p by a factor $(1 + \delta_\Delta)$. We take $\delta_\Delta = -0.57\delta m_\Delta/m_\Delta$ which gives a fair reproduction of the behavior of AV28 for both the deuteron and the virtual bound state as shown by the line in Table II labeled "δ_Δ". Using the same factor in AV18 again produces a larger rate of change.

We note that if the nucleon and Δ masses change at about the same rate, from whatever the underlying quark mass dependence, then the effect on the AV28 energies could be obtained by the sum of the m_N and m_Δ terms in Table II, which is not very different from the m_N term alone for AV14 and AV18 or from the sum of $m_N + \delta_N$ and δ_Δ terms. In fact, these corresponding sums of terms agree within 10–20% for all three models.

Increasing the pion mass reduces the regularized OPE tensor function $m_\pi^3 T(m_\pi r)$ at all values of r. The binding of the deuteron is primarily due to the tensor coupling, so Q is reduced and ΔQ is negative for all the models as shown by the line in Table II labeled "m_π (OPE)". The

TABLE III. $\Delta\mathcal{E}(m_H)$ for the AV14 Hamiltonian.

	^{3}H	^{3}He	^{4}He	^{5}He	^{6}Li	^{7}Li	^{7}Be	^{8}Be
m_N	6.00	6.44	3.97	4.58	5.25	5.60	5.88	5.10
$m_N + \delta_N$	12.32	13.17	9.03	10.38	11.35	12.74	13.41	11.71
δ_Δ	−7.35	−7.82	−5.89	−6.74	−7.10	−8.31	−8.76	−7.69
m_π (OPE)	−0.45	−0.50	−0.20	−0.24	−0.36	−0.30	−0.32	−0.23
m_π (+TPE-s)	−4.35	−4.66	−3.33	−3.87	−4.19	−4.83	−5.09	−4.38
m_π (+TPE-L)	−4.53	−4.85	−3.47	−4.04	−4.40	−5.06	−5.34	−4.59
m_V	29.36	31.30	23.60	27.09	28.98	33.72	35.55	30.98

value for AV28 is larger because of the multi-pion-exchange effects included through the generalized OPE potential. The AV14 and AV18 values are smaller and close together, the difference between them being proportional to the different $f_{\pi NN}^2$ coupling constants used in the two models.

Increasing m_π in the ${}^1S_0$ channel, which depends only on $m_\pi^3 Y(m_\pi r)$, has the effect of slightly increasing the attraction in the virtual bound state, making $\Delta(\epsilon_v)$ negative for the AV14 and AV18 models. However, in the AV28 model, the generalized OPE provides significant intermediate-range attraction $\propto [m_\pi^3 T(m_\pi r)]^2$, which is enough to reverse the sign of $\Delta(\epsilon_v)$ to be positive. As the AV14 and AV18 cases here are the only two out of seventeen in Table II that violate the relation between ΔQ and $\Delta(\epsilon_v)$ of Eq. (37), it appears that changing only the OPE part of a conventional NN potential like AV14 or AV18 is an incomplete representation of the physics in the singlet channel.

Changing m_π in the static TPE part of the interaction has a more dramatic effect than changing just the OPE part, as shown in Table II by the line labeled "m_π (+TPE-s)." The ΔQ increases by by a factor of 2.5–4 in the deuteron for the AV14 and AV18 models compared to OPE only, while for AV28 it increases by a smaller factor of 1.5. More dramatically, the AV14 and AV18 values for $\Delta\epsilon_v$ change sign and come into agreement with Eq. (37). The further addition of the nonstatic "m_π (+TPE-L)" terms makes no difference to the virtual bound state, as these operators do not contribute in the ${}^1S_0$ channel, and rather small changes in the deuteron.

Finally, increasing the heavy-meson mass m_V reduces the range of the Woods-Saxon repulsion and increases the binding of the deuteron, so ΔQ is positive. The reduced repulsion for the virtual bound state correspondingly makes $\Delta\epsilon_v$ negative.

In both the full-pion and heavy-meson exchanges, the AV18 has larger $\Delta\mathcal{E}$ values than AV14 or AV28. Again, this is probably due to the weaker OPE and compensatingly larger intermediate-range attraction and short-range repulsion.

B. Multinucleon energies

The multinucleon results for $\Delta\mathcal{E}(m_H)$ are given in Table III for AV14 and Table IV for AV18+UIX. For every nucleus, and for every m_H component, the signs are the same as for the deuteron. The relative sizes of the terms are also about the same as the deuteron, with the exception of the m_π (OPE) term. Because the light nuclei have approximately equal numbers of deuteron-like and ${}^1S_0$-like pairs [44], the $\Delta\mathcal{E}(m_H)$ are expected to be averages of the two sets of trends in Table II. The anomalous behavior of $\Delta\epsilon_v$ in the m_π (OPE) case discussed above causes these numbers to be much smaller in the multinucleon systems, and thus out of proportion compared to all the other terms. As for the deuteron, the multinucleon terms have a more rapid dependence with AV18+UIX than with AV14. However, the explicit m_π contribution from the three-nucleon force is very small.

IV. DEPENDENCE OF NUCLEAR BINDING ENERGIES AND BIG BANG NUCLEOSYNTHESIS ON QUARK MASS

As an example of how to incorporate our nuclear binding energy results with a specific prediction for hadronic mass variation, we utilize the results of a Dyson-Schwinger equation study of sigma terms in light-quark hadrons [27]. Equations (85–86) of that work gives the rate of hadron mass variation

TABLE IV. $\Delta\mathcal{E}(m_H)$ for the AV18+UIX Hamiltonian.

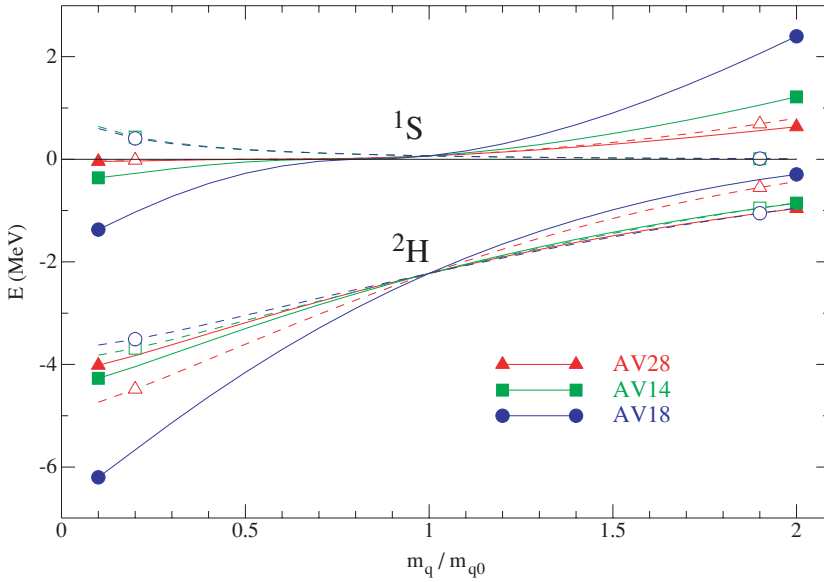|	^{3}H	^{3}He	^{4}He	^{5}He	^{6}Li	^{7}Li	^{7}Be	^{8}Be
m_N	6.07	6.54	3.99	4.51	5.12	5.24	5.49	4.81
$m_N + \delta_N$	16.56	17.73	11.86	13.31	14.41	15.53	16.29	14.36
δ_Δ	−12.20	−13.02	−9.16	−10.24	−10.80	−11.96	−12.56	−11.11
m_π (OPE)	−0.37	−0.42	−0.19	−0.24	−0.36	−0.29	−0.30	−0.23
m_π (+TPE-s)	−6.90	−7.38	−5.11	−5.82	−6.33	−6.95	−7.30	−6.34
m_π (+TPE-L)	−6.87	−7.36	−5.06	−5.75	−6.24	−6.84	−7.18	−6.24
m_π (+TNI)	−6.91	−7.40	−5.12	−5.82	−6.31	−6.91	−7.26	−6.31
m_V	47.98	51.23	36.34	40.87	43.48	48.11	50.53	44.40

FIG. 1. (Color online) Variation of two-nucleon energies with current-quark mass variation from DSE calculation: full calculation (solid lines) and with OPE modification only (dashed lines) for three different Argonne Hamiltonians. Virtual bound state energies are plotted as positive quantities; m_{q0} is the physical current-quark mass.

as a function of the average light current-quark mass $m_q = (m_u + m_d)/2$ as

$$\frac{\delta m_H}{m_H} = \frac{\sigma_H}{m_H} \frac{\delta m_q}{m_q} \quad (39)$$

with σ_H/m_H values of 0.498 for the pion, 0.030 for the ρ-meson, 0.043 for the ω-meson, 0.064 for the nucleon, and 0.041 for the Δ. The values for the ρ and ω-mesons were reduced to 0.021 and 0.034, respectively, in a subsequent study [28]. We will use an average of the ρ and ω terms of 0.03 for the variation of our short-range mass parameter m_V.

In Fig. 1 we show direct calculations for the two-nucleon states, i.e., the deuteron and $^1S_0(np)$ states, for a range of m_q values for all three Hamiltonians. The virtual bound state energies are plotted as a positive quantity; when the $^1S_0$ energy is negative it indicates a true bound state. The dashed lines show the results from changing only the pion mass in the OPE part of the interaction, corresponding to the line m_π (OPE) in Table II. To evaluate over this wide range of m_q, we use the Gell-Mann-Oakes-Renner (GMOR) relation $m_\pi^2 \propto m_q$.

The solid lines show the most complete calculation for each Hamiltonian. For the AV28 model this is the sum of the terms m_N, m_Δ, m_π (+TPE-L), and m_V, using GMOR for the pion and the DSE values above for the variation of all other m_H. For the AV14 and AV18 models, it is the sum of the terms $m_N + \delta_N, \delta_\Delta, m_\pi$ (+TPE-L), and m_V. As discussed in Sec. III A, the δ_N and δ_Δ effects are incorporated by multiplying the intermediate-range strength parameters I^p of Eq. (15) by a factor

$$(1 + \delta_N)(1 + \delta_\Delta) = \left(1 + 0.49 \frac{\delta m_N}{m_N}\right)\left(1 - 0.57 \frac{\delta m_\Delta}{m_\Delta}\right) \quad (40)$$

which is $\approx (1 + 0.008 \, \delta m_q/m_q)$ for the DSE values above.

At the OPE level, the AV14 and AV18 models show almost exactly the same behavior for the $^1S_0$ state, with a gradually increasing attraction as m_q increases, while for the deuteron they both show a more rapid decrease in binding, consistent with the results obtained in Refs. [23,24]. If these trends

continue, the deuteron will eventually move above the singlet state somewhere in the range 3–4 m_{q0}. The AV28 model has a somewhat more rapid dependence for the deuteron but its singlet state parallels the deuteron, becoming less attractive for larger m_q. In the other direction, the singlet state becomes a true bound state at $\approx 0.7 m_{q0}$, but it always remains above the deuteron. This different behavior is a consequence of the multipion exchange that is built into the AV28 model through the generalized OPE coupling to intermediate Δ's.

In all these models the deuteron is bound largely through the tensor coupling between the $^3S_1$ and $^3D_1 NN$ states. In the AV28 model, the singlet state gets a considerable part of its attraction through the tensor coupling between the $^1S_0 NN$ and intermediate $^5D_0 N\Delta$ states, and thus has a sensitivity to changes in the pion mass similar to the deuteron. This behavior of the singlet state, i.e., that it parallels the deuteron, is different from that predicted by chiral perturbation theory evaluated at the next-to-leading-order (NLO) in Ref. [30], which does not include the effect of the Δ. We expect that a higher-order chiral perturbation calculation that includes Δ degrees of freedom will come into qualitative agreement with our result.

For our most complete calculations, shown by the solid lines, the mass dependence of the energies is significantly steeper for both deuteron and singlet states, but they all are parallel and it appears the deuteron will remain the ground state for a very large range of m_q. The AV28 curves shift relatively little from the OPE-only values, while the AV14, which is essentially phase equivalent with AV28, gives very similar results. The biggest change and the most-rapid dependence is given by the AV18 model, with the most important contribution coming from its static two-pion-exchange terms, i.e., the line $m_\pi (+TPE - s)$ in Table II. The more rapid dependence is a consequence of the deeper intermediate-range attraction and stronger short-range repulsion, which in turn may be a consequence of the improved quality of AV18, i.e., that it is a better fit to more recent NN data.

The two-body energies can also be evaluated using Eq. (37) to combine the DSE values for $\delta m_H/m_H$ and the
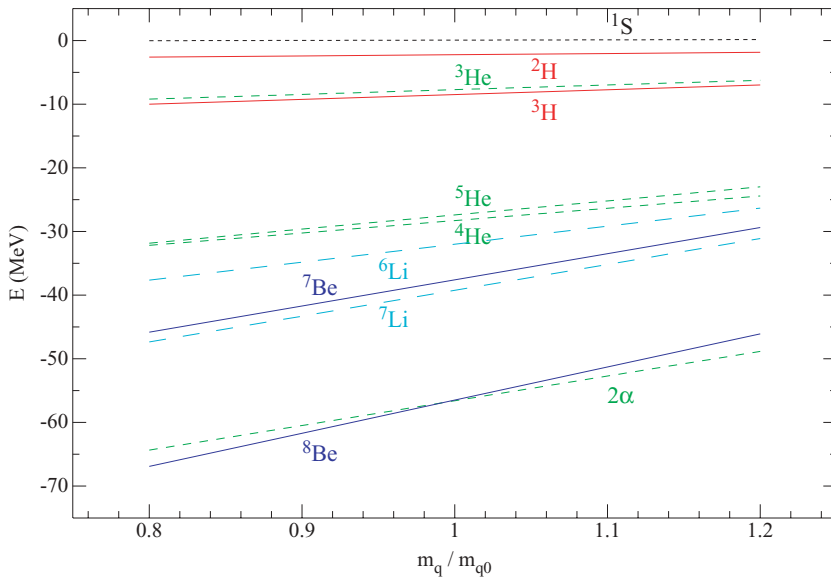
FIG. 2. (Color online) Variation of multinucleon energies with current-quark mass variation from DSE calculation for AV14 Hamiltonian.

dimensionless derivatives $\Delta\mathcal{E}(m_H)$ of Table II. This might not be expected to work for large changes in m_q, or where a state is barely bound or unbound. However, deuteron energies are reproduced for changes of ± 0.1 in $\delta m_q/m_q$ to 1% or better by Eq. (37).

The dependence of the multinucleon energies for the full calculation with DSE values is shown in Fig. 2 for AV14 and in Fig. 3 for AV18+UIX. These results have been calculated using Eq. (37) and the $\Delta\mathcal{E}(m_H)$ of Tables III and IV, respectively. The lines have been extended to $\delta m_q = \pm 0.2 m_q$ to show the trends, although the results are not expected to be completely linear over such a broad range. The values have been checked in a few cases by doing direct calculations and adjusting the variational parameters to reminimize the energy. For example, the ^{4}He energy can be lowered by 0.3–0.5 MeV

at either end of its line, but this change would hardly be visible at the scale shown.

The multinucleon energies parallel the deuteron, with generally increasing slope as the binding energy increases. (Similar results for the triton were found in Refs. [45,46].) The curves are steeper for AV18+UIX than for AV14. In either case it appears that the relative stability of all the nuclei will be preserved across a broad range of m_q values, with the exception of ^{8}Be. Here it appears that a decrease in m_q of ≈ 0.5% will lead to ^{8}Be stable against breakup into two α's for both Hamiltonians. A very weakly bound ($\sim$0.1 MeV) ^{8}Be might not have much of an impact on primordial nucleosynthesis because it would be easily photodisintegrated until quite late in the BBN epoch. A moderate binding ($\sim$1 MeV) could have a significantly more dramatic effect on the chemical evolution
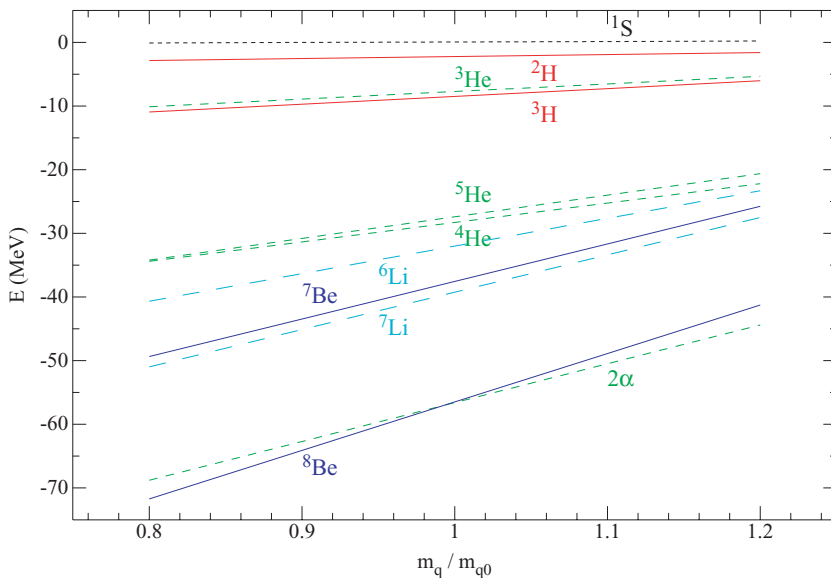

FIG. 3. (Color online) Variation of nuclear energies with current-quark mass variation from DSE calculation for AV18+UIX Hamiltonian.

TABLE V. Dimensionless derivatives $K = \frac{\delta E/E}{\delta m_q/m_q}$ of the energy over light quark mass m_q for the different Hamiltonians.

	$^1S_0(np)$	^{2}H	^{3}H	^{3}He	^{4}He	^{5}He	^{6}Li	^{7}Li	^{7}Be	^{8}Be
AV28	4.5	−0.75								
AV14	7.3	−0.84	−0.89	−0.96	−0.69	−0.81	−0.89	−1.03	−1.09	−0.92
AV18+UIX	11.4	−1.39	−1.44	−1.55	−1.08	−1.24	−1.36	−1.50	−1.57	−1.35

of the Universe by giving rise to the production of noticeable amounts of stable elements with $A = 9, 10$. If the bound state persisted to the era of star formation, it would presumably also have a significant effect on stellar evolution.

A summary of sensitivities of nuclear binding energies to the quark mass m_q, as given by the DSE hadronic mass variation, is presented in Table V for the different Hamiltonians. The total sensitivity K,

$$K = \frac{\delta E/E}{\delta m_q/m_q}, \qquad (41)$$

of deuterium binding energy to the light quark mass is $K_d = -1.39$ for the AV18 interaction, while the pion contribution ranges from $K_d^\pi = -0.70$ for the OPE contribution only to $K_d^\pi = -3.36$ when the full TPE is counted. This may be compared with the pion contribution $3 > K_d^\pi > -18$ from Ref. [9] and $K_d^\pi = -2.4$ from Ref. [24].

The result of Ref. [10] suggested that a reduced deuteron binding energy of $\Delta Q = -0.019 \pm 0.005$ would yield a better fit to observational data (the WMAP value of η and measured ^{2}H, ^{4}He, and ^{7}Li abundances) for big bang nucleosynthesis. This would correspond to an increase in the quark mass of $\delta X_q/X_q = 0.014 \pm 0.004$ (here $X_q = m_q/\Lambda_{QCD}$).

Dent, Stern, and Wetterich [11] calculated the sensitivity of BBN abundances for ^{2}H, ^{4}He and ^{7}Li to the variation of binding energies of ^{2,3}H, ^{3,4}He, ^{6,7}Li, and ^{7}Be in a linear approximation. We use the response matrix values in their Table I for m_N to B_{7Be} and multiply by the $\delta m_N/m_N$ and K values of our Table V to estimate the sensitivity of BBN yields to variation of the quark mass. If we compare to the ratio of observation and theoretically predicted abundances given in their Appendix B, we obtain the following equations for ^{2}H, ^{4}He, and ^{7}Li:

$$1 + 7.7x = \frac{2.8 \pm 0.4}{2.61 \pm 0.04} = 1.07 \pm 0.15, \qquad (42)$$

$$1 - 0.95x = \frac{0.249 \pm 0.009}{0.2478 \pm 0.0002} = 1.005 \pm 0.036, \qquad (43)$$

$$1 - 50x = \frac{1.5 \pm 0.5}{4.5 \pm 0.4} = 0.33 \pm 0.11, \qquad (44)$$

where $x = \delta X_q/X_q$. These equations yield 3 consistent values of x: 0.009 ± 0.019, -0.005 ± 0.038, and 0.013 ± 0.002. The statistically weighted average of $\delta X_q/X_q = 0.013 \pm 0.002$ is dominated by the ^{7}Li data. A more accurate calculation should take into account the effect of the ^{8}Be binding energy variation (which is not calculated in Ref. [11]), the variation of the virtual $^1S_0(np)$ level, and nonlinear corrections in x which are important for ^{7}Li. Allowing for the theoretical uncertainties

we should understand this BBN result as $\delta X_q/X_q = K \cdot (0.013 \pm 0.002)$ where $K \sim 1$ and the expected accuracy in K is about a factor of 2. Note that here we neglect effects of the strange quark mass variation. A rough estimate of these effects on BBN due to the deuteron binding energy variation was made in Refs. [9,10].

V. CONCLUSIONS

We have argued that there are several reasons to question the spatial and temporal invariance of various fundamental "constants" of nature, such as the fine structure constant α or a comparable strong interaction parameter $X_q = m_q/\Lambda_{QCD}$. The search for evidence of such variations is ongoing in areas as diverse as quasar absorption spectra, the Oklo natural nuclear reactor, and big bang nucleosynthesis.

In this work we have examined how nuclear binding energies depend on hadronic masses, including m_N, m_Δ, m_π, and a generic heavy meson m_V. We have done this by identifying the mass dependence in several realistic Hamiltonians—interactions that fit NN elastic scattering data and reproduce light nuclei binding energies reasonably well in quantum Monte Carlo calculations. By making small changes in the masses and reevaluating the energy, we have obtained the dimensionless derivatives of the energy with respect to variations in the hadronic masses.

We have combined these results with a specific prediction from a Dyson-Schwinger equation study of sigma terms in the light-quark hadrons for the hadronic mass dependence on the quark mass m_q. The pion mass changes most rapidly with changes in m_q, so we find that both the one- and two-pion exchange parts of the NN interaction are very important for the consequent variations in nuclear binding. With our most complete model, the $^1S_0$ virtual bound state and deuteron vary in concert; if X_q increases, they both become less bound, while if X_q decreases, they both become more bound. (We note that this result is in disagreement with chiral perturbation results at the NLO level which have $^1S_0$ and $^3S_1$ scattering varying antithetically.) The binding energies of $A = 3$–8 nuclei behave in the same manner, all moving up or down together, with a sensitivity K in the range -1 to -1.5.

Finally, we have folded these results with a study of the sensitivity of big bang nucleosynthesis to variations in nuclear binding. We find that a small increase in the quark mass of order 1% at the time of BBN is sufficient by itself to resolve existing discrepancies between theoretical and measured abundances of ^{2}H, ^{4}He, and ^{7}Li.

[1] W. J. Marciano, Phys. Rev. Lett. **52**, 489 (1984); X. Calmet and H. Fritzsch, Eur. Phys. J. C **24**, 639 (2002); P. Langacker, G. Segré, and M. J. Strassler, Phys. Lett. **B528**, 121 (2002); T. Dent and M. Fairbairn, Nucl. Phys. **B653**, 256 (2003); C. Wetterich, JCAP 10 (2003) 002; Phys. Lett. **B561**, 10 (2003).

[2] J.-P. Uzan, Rev. Mod. Phys. **75**, 403 (2003).

[3] T. Damour and K. Nordtvedt, Phys. Rev. Lett. **70**, 2217 (1993); Phys. Rev. D **48**, 3436 (1993).

[4] T. Damour and A. M. Polyakov, Nucl. Phys. **B423**, 532 (1994).

[5] J. D. Bekenstein, Phys. Rev. D **25**, 1527 (1982).

[6] C. Wetterich, Nucl. Phys. **B302**, 645 (1988).

[7] H. B. Sandvik, J. D. Barrow, and J. Magueijo, Phys. Rev. Lett. **88**, 031302 (2002).

[8] K. A. Olive and M. Pospelov, Phys. Rev. D **65**, 085044 (2002).

[9] V. V. Flambaum and E. V. Shuryak, Phys. Rev. D **65**, 103503 (2002); V. F. Dmitriev and V. V. Flambaum, *ibid.* **67**, 063513 (2003); V. V. Flambaum and E. V. Shuryak, *ibid.* **67**, 083507 (2003).

[10] V. F. Dmitriev, V. V. Flambaum, and J. K. Webb, Phys. Rev. D **69**, 063506 (2004).

[11] T. Dent, S. Stern, C. Wetterich, Phys. Rev. D **76**, 063513 (2007).

[12] A. Coc, N. J. Nunes, K. A. Olive, J.-P. Uzan, and E. Vangioni, Phys. Rev. D **76**, 023511 (2007).

[13] J. P. Kneller and G. C. McLaughlin, Phys. Rev. D **68**, 103508 (2003).

[14] S. K. Lamoreaux and J. R. Torgerson, Phys. Rev. D **69**, 121701(R) (2004).

[15] C. R. Gould, E. I. Sharapov, and S. K. Lamoreaux, Phys. Rev. C **74**, 024607 (2006); Yu. V. Petrov, A. I. Nazarov, M. S. Onegin, V. Yu. Petrov, and E. G. Sakhnovsky, *ibid.* **74**, 064610 (2006); Y. Fujii, A. Iwamoto, T. Fukahori, T. Ohnuki, M. Nakagawa, H. Hidaka, Y. Oura, and P. Möller, Nucl. Phys. **B573**, 377 (2000).

[16] A. Ivanchik, P. Petitjean, D. Varshalovich, B. Aracil, R. Srianand, H. Chand, C. Ledoux, and P. Boissé, Astron. Astrophys. **440**, 45 (2005); E. Reinhold, R. Buning, U. Hollenstein, A. Ivanchik, P. Petitjean, and W. Ubachs, Phys. Rev. Lett. **96**, 151101 (2006).

[17] P. Tzanavaris, J. K. Webb, M. T. Murphy, V. V. Flambaum, and S. J. Curran, Phys. Rev. Lett. **95**, 041301 (2005).

[18] V. V. Flambaum and M. G. Kozlov, Phys. Rev. Lett. **98**, 240801 (2007).

[19] V. V. Flambaum and A. F. Tedesco, Phys. Rev. C **73**, 055501 (2006).

[20] V. V. Flambaum, Phys. Rev. Lett. **97**, 092502 (2006).

[21] E. Peik and Chr. Tamm, Europhys. Lett. **61**, 181 (2003).

[22] V. V. Flambaum, arXiv:0705.3704v2 [physics.atom-ph].

[23] S. R. Beane and M. J. Savage, Nucl. Phys. **A713**, 148 (2003).

[24] E. Epelbaum, Ulf-G. Meißner, and W. Glöckle, Nucl. Phys. **A714**, 535 (2003).

[25] V. V. Flambaum, D. B. Leinweber, A. W. Thomas, and R. D. Young, Phys. Rev. D **69**, 115006 (2004).

[26] W. Armour, C. R. Allton, D. B. Leinweber, A. W. Thomas, and R. D. Young, J. Phys. G **32**, 971 (2006).

[27] V. V. Flambaum, A. Höll, P. Jaikumar, C. D. Roberts, and S. V. Wright, Few-Body Syst. **38**, 31 (2006).

[28] A. Höll, P. Maris, C. D. Roberts, and S. V. Wright, arXiv:nucl-th/0512048v1.

[29] R. B. Wiringa and S. C. Pieper, Phys. Rev. Lett. **89**, 182501 (2002).

[30] S. R. Beane, P. F. Bedaque, K. Orginos, and M. J. Savage, Phys. Rev. Lett. **97**, 012001 (2006).

[31] R. B. Wiringa, R. A. Smith, and T. L. Ainsworth, Phys. Rev. C **29**, 1207 (1984).

[32] R. B. Wiringa, V. G. J. Stoks, and R. Schiavilla, Phys. Rev. C **51**, 38 (1995).

[33] B. S. Pudliner, V. R. Pandharipande, J. Carlson, and R. B. Wiringa, Phys. Rev. Lett. **74**, 4396 (1995).

[34] R. A. Arndt and L. D. Roper, Scattering Analyses Interactive Dial-in (SAID) program of the Center for Analysis of Particle Scattering, Department of Physics, Virginia Polytechnic Institute and State University.

[35] A. Picklesimer, R. A. Rice, and R. Brandenburg, Phys. Rev. C **46**, 1178 (1992).

[36] R. B. Wiringa, Lect. Notes in Phys. **198**, 44 (1984).

[37] R. B. Wiringa, Phys. Rev. C **43**, 1585 (1991).

[38] S. C. Pieper, R. B. Wiringa, and V. R. Pandharipande, Phys. Rev. C **46**, 1741 (1992).

[39] R. B. Wiringa, V. Fiks, and A. Fabrocini, Phys. Rev. C **38**, 1010 (1988).

[40] V. G. J. Stoks, R. A. M. Klomp, M. C. M. Rentmeester, and J. J. de Swart, Phys. Rev. C **48**, 792 (1993).

[41] S. C. Pieper and R. B. Wiringa, Annu. Rev. Nucl. Part. Sci. **51**, 53 (2001).

[42] A. Akmal and V. R. Pandharipande, Phys. Rev. C **56**, 2261 (1997).

[43] J. L. Forest, V. R. Pandharipande, and J. L. Friar, Phys. Rev. C **52**, 568 (1995).

[44] R. B. Wiringa, Phys. Rev. C **73**, 034317 (2006).

[45] E. Epelbaum, H.-W. Hammer, Ulf-G. Meißner, and A. Nogga, Eur. Phys. J. C **48**, 169 (2006).

[46] H.-W. Hammer, D. R. Phillips, and L. Platter, Eur. Phys. J. A **32**, 335 (2007).